Dalton Transactions

PAPER

View Article Online
View Journal | View Issue

Cite this: *Dalton Trans.*, 2014, **43**, 13434

The effect of the regioisomeric naphthalimide acetylide ligands on the photophysical properties of *N^N* Pt(II) bisacetylide complexes†

Lianlian Liu, Caishun Zhang and Jianzhang Zhao*

Received 11th June 2014,
Accepted 13th July 2014

DOI: 10.1039/c4dt01732c

www.rsc.org/dalton

Two *N^N* Pt(II) bis(acetylide) complexes **Pt-1** and **Pt-2** with regioisomeric amino NI acetylide ligands (**L-1** and **L-2**, **L-1** = 5-amino-4-ethylnaphthaleneimide; **L-2** = 3-amino-4-ethylnaphthaleneimide) were prepared. The photophysical properties of the complexes were studied by steady state and time-resolved spectroscopy. The two complexes with regioisomeric ligands (**Pt-1** and **Pt-2**) show different photophysical properties such as maximal absorption wavelength (485 nm *vs.* 465 nm), triplet excited state lifetimes (23.7 μs *vs.* 0.9 μs), and different solvent-polarity dependences of the emission properties. The absorption of the complexes is red-shifted as compared with the previously reported Pt(II) complex containing the 4-ethylnaphthaleneimide ligand. The two complexes with regioisomeric NI ligands were used as triplet photosensitizers for triplet–triplet annihilation (TTA) upconversion; drastically different upconversion quantum yields (15.0% *vs.* 1.1%) were observed. Our results are useful for designing new visible light-harvesting Pt(II) bisacetylide complexes as triplet photosensitizers which can be used in areas such as photocatalysis, photodynamic therapy and TTA upconversion.

Introduction

N^N Pt(II) bis(acetylide) complexes (*N^N* stands for one bidentate ligand coordinating through two nitrogen atoms, the typical example of these ligands is 2,2′-bipyridine) have attracted much attention due to their readily tunable photophysical properties using either different acetylide ligands or the *N^N* coordination ligands.[1–7] Recently these complexes have been used for photocatalytic hydrogen (H_2) production,[8] photoredox catalytic organic reactions,[9] photo-induced charge separation,[10] phosphorescent molecular probes,[2,11–13] non-linear optics,[14,15] and triplet–triplet annihilation upconversion.[16–19] Concerning most of these applications, intermolecular energy or electron transfer is typical, and the visible light-harvesting ability of the complexes is crucial.[20,21] Strong visible light-harvesting will enhance the production of the triplet excited state, because the concentration of the molecules at the excited state is proportional to the photons absorbed by the compound. On the other hand, the triplet excited state lifetime is also crucial for the applications because a long-lived triplet excited state is able to enhance the intermolecular electron transfer or energy transfer. However, conventional Pt(II) acetylide complexes show weak absorption in the visible region and the triplet excited state lifetime is short (a few microseconds).[1,14,15,20,21] Therefore, much room is left for preparation of visible light-harvesting Pt(II) bisacetylide complexes showing a long-lived triplet excited state and for full exploration of the potential applications of these interesting compounds.

In order to enhance the visible light absorption, a straightforward method is to attach an organic visible light-harvesting chromophore to the Pt(II) coordination center.[20,22–26] However, efficient intersystem crossing (ISC) or intramolecular energy transfer must be implemented otherwise the production of the triplet excited state will not be enhanced. Moreover, the photophysical properties of the complexes are elusive. For example, previously perylenebisimide (PBI) was attached to the Pt(II) coordination center. The complexes showed enhanced absorption in the visible region. Interestingly, the triplet excited state lifetime was very short (246 ns).[27] On the other hand, pyrenyl acetylides were used to prepare the *N^N* Pt(II) bisacetylide complex, and a long-lived triplet excited state was observed (48.5 μs),[28] but the complex showed absorption only in UV and blue regions. Recently we prepared the naphthalimide acetylide-containing Pt(II) complex, which shows a long-lived triplet excited state, but the complex shows absorption only in the blue spectral region.[29,30] We also used regioisomeric NI ligands to prepare cyclometalated Ir(III) complexes.[31]

State Key Laboratory of Fine Chemicals, School of Chemical Engineering, Dalian University of Technology, E 208 Western Campus, 2 Ling-Gong Road, Dalian 116012, P.R. China. E-mail: zhaojzh@dlut.edu.cn; http://finechem.dlut.edu.cn/photochem

†Electronic supplementary information (ESI) available. See DOI: 10.1039/c4dt01732c

In order to prepare Pt(II) complexes showing red-shifted absorption and a long-lived triplet excited state, herein we report the preparation of *N^N* Pt(II) complexes with amino NI acetylide ligands (Scheme 1). Two regioisomers were used, 5-amino-4-ethylnaphthaleneimide and 3-amino-4-ethylnaphthaleneimide. The corresponding Pt(II) complexes **Pt-1** and **Pt-2** show red-shifted absorption in the region 450–550 nm as compared with the previously reported Pt(II) complexes. With steady state and time-resolved spectroscopy, as well as DFT calculations, we found that at RT the complexes show near IR phosphorescence due to the amino-NI ligand in the complex. A long-lived triplet excited state (23.7 μs) was also observed. Interestingly, **Pt-1** and **Pt-2** show different photophysical properties, such as absorption wavelength, phosphorescence emission and lifetimes, as well as the dependence of the emission properties on the solvent polarity. The complexes were used as triplet photosensitizers for TTA upconversion. Improved upconversion was observed compared with the previously reported NI-containing Pt(II) complexes. Our studies indicated the significant effect of the regioisomers of the

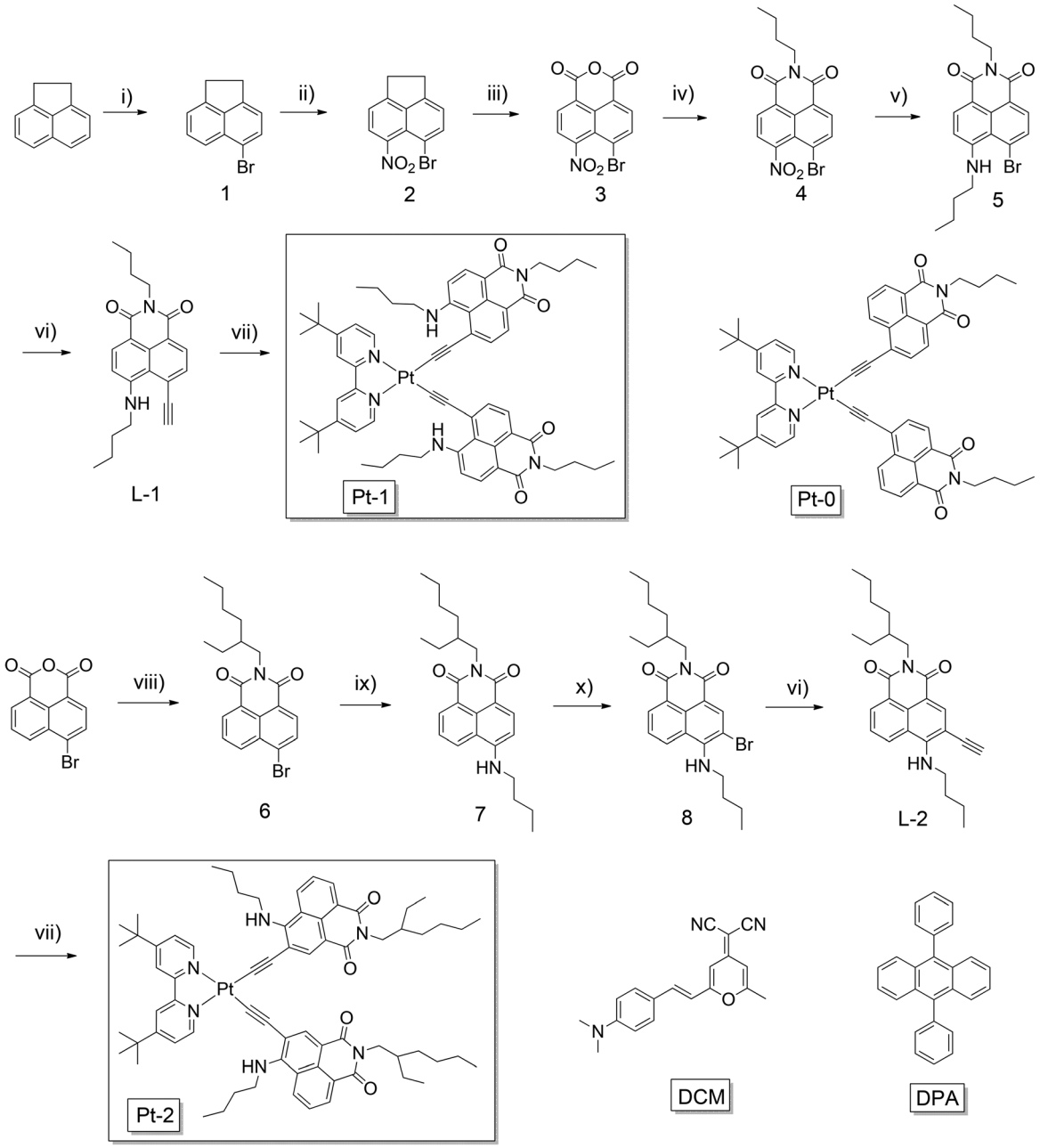

Scheme 1 Synthesis of the complexes **Pt-1** and **Pt-2**. (i) NBS, DMF, RT, 3 h; (ii) fuming nitric acid, AcOH, r.t., 10 h; (iii) $Na_2Cr_2O_7{\cdot}2H_2O$, AcOH, reflux, 3 h; (iv) *n*-butylamine, ethanol, reflux, 40 min; (v) *n*-butylamine, $CH_3OCH_2CH_2OH$, 80 °C, 1 h; (vi) trimethylsilylacetylene, $Pd(PPh_3)_2Cl_2$, PPh_3, CuI, NEt_3, Ar, reflux, 6 h; K_2CO_3, THF–MeOH, r.t., 0.5 h; (vii) Pt(dbbpy)Cl_2, CuI, diisopropylamine, CH_2Cl_2, r.t., 20 h; (viii) 2-ethylhexylamine, ethanol, reflux, 8 h; (ix) *n*-butylamine, $CH_3OCH_2CH_2OH$, reflux, 8 h; (x) Br_2, CH_2Cl_2, r.t., 12 h.

amino-NI ligands on the photophysical properties of the complexes, and the results will be useful for preparation of visible light-harvesting Pt(II) bisacetylide complexes and for the application of these complexes in areas such photocatalysis and TTA upconversion.

Experimental

Materials and reagents

All the reagents were analytically pure and were used as received. Solvents were dried and distilled before use.

Analytical measurements

NMR spectra were recorded on a 400 MHz Varian Unity Inova spectrophotometer (with TMS as the standard). Mass spectra were recorded with a Q-TOF Micro MS spectrometer. UV-Vis absorption spectra were measured with an Agilent 8453 UV-vis spectrophotometer. Fluorescence spectra and upconversion were recorded on a Shimadzu RF-5301PC spectrofluorometer. Phosphorescence quantum yields were measured with 4-(dicyanomethylene)-2-methyl-6-(4-dimethylaminostyryl)-4*H*-pyran (DCM) as the standard (Φ = 0.1 in CH_2Cl_2). Luminescence lifetimes were measured on an OB920 luminescence lifetime spectrometer (Edinburgh Instruments, UK) and an FLS920 spectrofluorometer (Edinburgh Instruments, UK). The quantum yield of singlet oxygen was measured with *meso*-tetraphenylporphyrin (TPP, Φ_Δ = 0.62 in CH_2Cl_2) and Rose Bengal (Φ_Δ = 0.8 in methanol) as standards.

Synthesis

Compound 1. A solution of *N*-bromosuccinimide (NBS. 3.6 g, 20.2 mmol) in DMF (10 mL) was added dropwise to a solution of acenaphthene (3.1 g, 20.1 mmol) in DMF (10 mL) at room temperature (RT). After 3 h, the solution was poured into ice water to give a yellow solid which was filtered, washed with water, and then dried in air. The product was further purified by column chromatography (silica gel, petroleum ether) to give **1** as a white solid (4.36 g), yield: 93.6%. EI-HRMS: calcd ($[C_{12}H_9Br]^+$) *m*/*z* = 231.9888, found *m*/*z* = 231.9881. No ^{1}H NMR spectrum was recorded due to the poor solubility.

Compound 2. A solution of fuming nitric acid (1 mL) in glacial acetic acid (2 mL) was added dropwise to a solution of compound **1** (1.12 g, 4.4 mmol) in glacial acetic acid (4 mL) in an ice-water bath. Then the reaction mixture was stirred at RT for 10 h. The product was filtered and purified by recrystallization with glacial acetic acid to give **2** as a yellow acicular crystal (0.65 g), yield: 53.4%. ^{1}H NMR (400 MHz, $CDCl_3$): 7.83 (d, 1H, *J* = 8.0 Hz), 7.72 (d, 1H, *J* = 8.0 Hz), 7.32–7.26 (m, 2H), 3.44–3.42 (m, 4H). EI-HRMS: calcd ($[C_{12}H_8NO_2Br]^+$) *m*/*z* = 276.9738, found *m*/*z* = 276.9691.

Compound 3. Compound **2** (1.21 g, 4.4 mmol) was added to a solution of $Na_2Cr_2O_7{\cdot}2H_2O$ (3.0 g, 10.1 mmol) in glacial acetic acid (12 mL) at RT. The mixture was refluxed and stirred for 3 h. Then the mixture was poured into ice water and filtered, and then the solid was washed with water and a little glacial acetic acid. The product was further purified by recrystallization with glacial acetic acid to give **3** as a dark yellow crystal (0.93 g), yield: 65.4%. ^{1}H NMR (400 MHz, DMSO): 8.68 (d, 1H, *J* = 4.0 Hz), 8.49–8.44 (m, 3H). EI-HRMS: calcd ($[C_{12}H_4NO_5Br]^+$) *m*/*z* = 320.9273, found *m*/*z* = 320.9283.

Compound 4. A solution of compound **3** (0.14 g, 0.43 mmol) in ethanol (13 mL) was heated to reflux. A moment later the solution was cooled to 50 °C, and a solution of *n*-butylamine (0.043 mL, 0.032 g, 0.43 mmol) in ethanol (5 mL) was added dropwise. The mixture was refluxed and stirred for additional 40 min. The solvent was removed under vacuum and the residue was further purified by column chromatography (silica gel, CH_2Cl_2) to give **4** as a yellow solid (120.2 mg), yield: 74.0%. ^{1}H NMR (400 MHz, $CDCl_3$): 8.69 (d, 1H, *J* = 8.0 Hz), 8.50 (d, 1H, *J* = 8.0 Hz), 8.20 (d, 1H, *J* = 8.0 Hz), 7.91 (d, 1H, *J* = 8.0 Hz), 4.15 (t, 2H, *J* = 8.0 Hz), 1.75–1.67 (m, 2H), 1.47–1.36 (m, 2H), 0.97 (t, 3H, *J* = 8.0 Hz).

Compound 5. *N*-Butylamine (0.034 mL, 24.7 mg, 0.34 mmol) was added to a solution of **4** (106.2 mg, 0.28 mmol) in ethylene glycol monomethyl ether ($CH_3OCH_2CH_3$, 10 mL) at 30 °C. Then the reaction mixture was heated to 80 °C and stirred for 1 h. The residue was filtered, and further purified by column chromatography (silica gel, CH_2Cl_2–CH_3OH, 100 : 1, v/v) to give **5** as a yellow solid (70.7 mg), yield: 62.6%. ^{1}H NMR (400 MHz, $CDCl_3$): 8.46 (d, 1H, *J* = 8.0 Hz), 8.31 (d, 1H, *J* = 8.0 Hz), 7.79 (d, 1H, *J* = 8.0 Hz), 7.58 (s, 1H), 6.71 (d, 1H, *J* = 8.0 Hz), 4.12 (t, 2H, *J* = 8.0 Hz), 3.34 (t, 2H, *J* = 8.0 Hz), 1.87–1.81 (m, 2H), 1.73–1.66 (m, 2H), 1.60–1.54 (m, 2H), 1.46–1.40 (m, 2H), 1.02 (t, 3H, *J* = 8.0 Hz), 0.95 (t, 3H, *J* = 8.0 Hz). MALDI-HRMS: calcd ($[C_{20}H_{23}N_2O_2Br + H]^+$) *m*/*z* = 403.1021, found *m*/*z* = 403.1043.

Compound L-1. Under an Ar atmosphere, $Pd(PPh_3)_2Cl_2$ (14.8 mg, 0.021 mmol), PPh_3 (11.1 mg, 0.042 mmol) and CuI (8.2 mg, 0.043 mmol) were added to a solution of **5** (169.4 mg, 0.42 mmol) in a mixed solvent of THF–Et_3N (12 mL/4 mL). Trimethylsilylacetylene (0.3 mL, 124.1 mg, 1.26 mmol) was added *via* a syringe. The mixture was stirred at 75 °C for 6 h. After the addition of water, CH_2Cl_2 was added to extract the product (3 × 25 mL). The organic phase was dried over anhydrous Na_2SO_4, filtered and the solvent was removed under reduced pressure. The residue was further purified by column chromatography (silica gel, CH_2Cl_2–CH_3OH = 100 : 1, v/v) to give a light red solid (143.8 mg), yield: 81.2%. K_2CO_3 (138.0 mg, 1.0 mmol) was added to a solution of the above trimethylsilane protected intermediate (140.2 mg, 0.33 mmol) in a mixed solvent CH_2Cl_2–MeOH (10 mL/5 mL). The mixture was stirred at RT for 30 min. After the addition of water, CH_2Cl_2 was added to extract the product (3 × 30 mL). The organic phase was dried over anhydrous Na_2SO_4, filtered and the solvent was evaporated under reduced pressure. The residue was further purified by column chromatography (silica gel, CH_2Cl_2–CH_3OH = 100 : 1, v/v) to give **L-1** as a light red solid (98.3 mg), yield: 85.5%. ^{1}H NMR (400 MHz, $CDCl_3$): 8.49–8.44 (m, 2H), 8.05 (s, 1H), 7.75 (d, 1H, *J* = 8.0 Hz), 6.66 (d, 1H, *J* = 8.0 Hz), 4.13 (t, 2H, *J* = 8.0 Hz), 3.88 (s, 1H), 3.35 (s, 1H), 1.82–1.41 (m, 8H), 1.04–0.95 (m, 6H). ^{13}C NMR (100 MHz, $CDCl_3$): 164.3, 164.1, 151.1, 135.1, 133.0, 131.0, 130.0, 123.8, 121.6, 119.2,

109.6, 105.2, 87.8, 84.4, 43.9, 40.2, 30.6, 30.4, 20.6, 14.1, 14.0 ppm. EI-HRMS: calcd ($[C_{22}H_{24}N_2O_2]^+$) m/z = 348.1838, found m/z = 348.1848.

Complex Pt-1. Pt(dbbpy)Cl_2 (25.0 mg, 0.047 mmol), CuI (5 mg, 0.09 mmol) and diisopropylamine (2 mL) were dissolved in CH_2Cl_2 (5 mL); the mixture was stirred for 10 min. Under Ar, **L-1** (49.1 mg, 0.14 mmol) was added and the mixture was stirred at RT overnight. After complete consumption of the starting material, the solvent was evaporated under reduced pressure, and the residue was purified by column chromatography (silica gel, CH_2Cl_2–CH_3OH = 60 : 1, v/v) to give **Pt-1** as a dark red solid (21.8 mg), yield: 40.0%. ^{1}H NMR (400 MHz, $CDCl_3$): 9.52 (d, 1H, J = 8.0 Hz), 8.46 (d, 1H, J = 8.0 Hz), 8.40 (d, 1H, J = 8.0 Hz), 8.07 (s, 1H), 7.73–7.69 (m, 2H), 6.59 (d, 1H, J = 8.0 Hz), 4.14 (t, 2H, J = 8.0 Hz), 3.21 (t, 2H, J = 8.0 Hz), 1.73–1.64 (m, 4H), 1.49–1.42 (m, 11H), 1.16–1.11 (m, 2H), 0.95 (t, 3H, J = 8.0 Hz), 0.57 (t, 3H, J = 8.0 Hz). ^{13}C NMR (100 MHz, $CDCl_3$): 164.9, 164.8, 164.3, 156.1, 152.5, 151.1, 134.8, 131.4, 131.1, 130.1, 128.9, 125.3, 120.1, 119.3, 119.2, 108.1, 104.0, 103.6, 103.1, 43.5, 39.9, 36.1, 30.4, 30.3, 30.2, 29.7, 20.5, 20.4, 13.9, 13.7 ppm. MALDI-HRMS: calcd ($[C_{62}H_{70}N_6O_2Pt]^-$) m/z = 1157.5106, found m/z = 1157.5027.

Compound 6. 4-Bromo-1,8-naphthalene dicarboxylic anhydride (1.0 g, 3.65 mmol) and 2-ethylhexylamine (0.8 g, 7.3 mmol) were dissolved in ethanol (100 mL). The mixture was refluxed for 8 h. Then the solvent was evaporated under reduced pressure, and the residue was purified by column chromatography (silica gel, CH_2Cl_2–petroleum ether = 1 : 2) to give **6** as a light yellow solid (1.1 g), yield: 80.0%. ^{1}H NMR (400 MHz, $CDCl_3$) 8.63–8.65 (d, 1H, J = 7.4 Hz), 8.53–8.55 (d, 1H, J = 8.5 Hz), 8.38–8.40 (d, 1H, J = 8.0 Hz), 8.01–8.03 (d, 1H, J = 7.9 Hz), 7.81–7.85 (t, 1H, J = 8.0 Hz), 4.05–4.16 (m, 2H), 1.88–1.98 (m, 1H), 1.29–1.41 (m, 8H), 0.86–0.95 (m, 6H). MALDI-HRMS: calcd ($[C_{20}H_{22}NO_2Br + H]^+$) m/z = 388.0912, found m/z = 388.0890.

Compound 7. Compound **6** (1.0 g, 2.64 mmol) and *n*-butylamine (1.3 mL, 962.0 mg, 13.2 mmol) were dissolved in $CH_3OCH_2CH_2OH$ (18 mL). Then the mixture was refluxed for 8 h. Water was added and CH_2Cl_2 was added to extract the product (3 × 25 mL). The combined organic layer was dried over anhydrous Na_2SO_4. After solvent was evaporated under reduced pressure, the residue was purified by column chromatography (silica gel, CH_2Cl_2) to give **7** as a light yellow solid (42.7 mg), yield: 40.2%. ^{1}H NMR (400 MHz, $CDCl_3$): 8.60 (d, 1H), 8.48 (d, 1H), 8.10 (s, 1H), 7.61–7.65 (m, 1H), 6.74 (s, 1H), 4.05–4.15 (m, 2H), 3.44 (t, 2H), 1.91–1.98 (m, 1H), 1.77–1.84 (m, 2H), 1.49–1.58 (m, 2H), 1.26–1.40 (m, 8H), 1.04 (t, 3H), 0.85–0.94 (m, 6H). EI-HRMS: calcd ($[C_{24}H_{32}N_2O_2]^+$) m/z = 380.2464, found m/z = 380.2471.

Compound 8. Br_2 (1.0 mL, 249.5 mg, 1.6 mmol) in anhydrous CH_2Cl_2 (10 mL) was added dropwise to a solution of **7** (200.0 mg, 0.53 mmol) in CH_2Cl_2 (10 mL) at RT, and stirred for 12 h. Then the solvent was removed under reduced pressure, and the residue was purified by column chromatography (silica gel, CH_2Cl_2–petroleum ether = 2 : 1) to give **8** as a yellow solid (296.4 mg), yield: 60.2%. ^{1}H NMR (400 MHz, $CDCl_3$): 8.64 (s, 1H), 8.59 (d, 2H), 8.50 (d, 2H), 7.65 (t, 1H), 4.03–4.14 (m, 2H), 3.65 (t, 2H), 1.89–1.95 (m, 1H), 1.71–1.79 (m, 2H), 1.29–1.48 (m, 10H), 0.86–0.98 (m, 9H). MALDI-HRMS: calcd ($[C_{24}H_{31}N_2O_2Br + H]^+$) m/z = 459.1647, found m/z = 459.1607.

Compound L-2. The synthetic procedure is similar to that of **L-1**, except that compound **8** (102.7 mg, 0.22 mmol) was used. The residue was further purified by column chromatography (silica gel, CH_2Cl_2–petroleum ether = 2 : 1, v/v) to give **L-2** as a yellow solid (69.1 mg), yield: 77.6%. ^{1}H NMR (400 MHz, $CDCl_3$): 8.56 (d, 1H, J = 8.0 Hz), 8.52 (s, 1H), 8.39 (d, 1H, J = 8.0 Hz), 7.63–7.59 (m, 1H), 5.54 (s, 1H), 4.12–4.06 (m, 2H), 3.86–3.81 (m, 2H), 3.52 (s, 1H), 1.94–1.91 (m, 1H), 1.77–1.72 (m, 2H), 1.52–1.29 (m, 10H), 1.00–0.86 (m, 9H). ^{13}C NMR (100 MHz, $CDCl_3$): 164.9, 163.8, 153.8, 136.8, 132.0, 130.5, 130.0, 125.0, 123.3, 121.7, 112.2, 104.2, 84.0, 80.6, 49.4, 44.1, 38.1, 33.6, 30.9, 28.9, 24.2, 23.3, 20.1, 14.3, 14.0, 10.9 ppm. EI-HRMS: calcd ($[C_{26}H_{32}N_2O_2 + H]^+$) m/z = 405.2542, found m/z = 405.2556.

Complex Pt-2. The synthetic procedure is similar to that of **Pt-1**, except that **L-2** (52.0 mg, 0.13 mmol) was used. The crude product was further purified by column chromatography (silica gel, CH_2Cl_2–CH_3OH = 150 : 1, v/v) to give **Pt-2** as a red solid (23.3 mg), yield: 42.3%. ^{1}H NMR (400 MHz, $CDCl_3$): 9.69 (d, 1H, J = 8.0 Hz), 8.64 (s, 1H), 8.53–8.49 (m, 1H), 8.04 (s, 1H), 7.72 (d, 1H, J = 8.0 Hz), 7.54–7.50 (m, 1H), 6.61 (s, 1H), 4.19–4.08 (m, 2H), 3.72–3.68 (m, 2H), 1.99–1.96 (m, 1H), 1.67–1.60 (m, 2H), 1.49–1.18 (m, 19H), 0.96–0.87 (m, 6H), 0.53 (t, 3H, J = 8.0 Hz). ^{13}C NMR (100 MHz, $CDCl_3$): 165.4, 164.6, 164.3, 156.3, 154.0, 151.4, 135.4, 131.1, 130.9, 129.7, 125.2, 123.7, 123.0, 120.9, 119.1, 111.2, 110.5, 96.9, 95.0, 49.8, 44.1, 38.1, 36.1, 33.3, 31.0, 30.4, 29.9, 29.0, 24.3, 23.3, 20.1, 14.3, 13.6, 10.9 ppm. MALDI-HRMS: calcd ($[C_{70}H_{86}N_6O_4Pt - H]^+$) m/z = 1268.6280, found m/z = 1268.6373.

Triplet–triplet annihilation upconversion

A diode pumped solid state (DPSS) continuous laser (473 nm and 532 nm) was used as the excitation source for the upconversion. The diameter of the 473 nm and 532 nm laser spot is *ca.* 3 mm. The power of the laser beam was measured with a VLP-2000 pyroelectric laser power meter. For the upconversion experiments, the mixed solution of the compound (triplet photosensitizers) and 9,10-diphenylanthracene (DPA) was degassed with N_2 for at least 15 min. The upconverted fluorescence of DPA was observed with a Shimadzu RF-5301PC spectrofluorometer. In order to repress the scattered laser, a small black box was put behind the fluorescent cuvette to dump the laser beam. The upconversion quantum yields (Φ_{UC}) were determined with the prompt fluorescence of 4-dicyanomethylene-2-methyl-6-(*p*(dimethylamino)styryl)-4*H*-pyran (DCM) as the luminescence quantum yield standard (Φ_F = 10% in CH_2Cl_2). The upconversion quantum yields were calculated using eqn (1), where Φ_{UC}, A_{sam}, I_{sam} and η_{sam} represent the quantum yield, absorbance, integrated photoluminescence intensity and refractive index of the solvents (where the subscript "std" stands for the standard used in the measurement of the quantum yield and "sam" stands for the samples to be

measured). The equation is multiplied by a factor of 2 in order to set the maximum quantum yield to unity.[16] All these data were independently measured three times (with different sample solutions).

$$\Phi_{UC} = 2\Phi_{std}\left(\frac{A_{std}}{A_{sam}}\right)\left(\frac{I_{sam}}{I_{std}}\right)\left(\frac{\eta_{sam}}{\eta_{std}}\right)^2 \quad (1)$$

All these data were independently measured three times. The CIE coordinates (x, y) of the emission of the sensitizers alone and the emission of the upconversion were derived from the emission spectra with the software of CIE color matching linear algebra.

DFT calculations

Density functional theory (DFT) calculations were used for optimization of both singlet and triplet states. The energy level of the T_1 state (energy gap between S_0 and T_1 states) was calculated with time-dependent DFT (TDDFT), based on the optimized singlet ground state geometries (S_0 state). All the calculations were performed with Gaussian 09W.[32]

Results and discussion

Design and synthesis of the complexes

Naphthalimide is a versatile chromophore and has been widely used in construction of molecular arrays and fluorescent molecular probes or fluorophores.[33–36] In comparison, the application of NI derivatives in the triplet excited state manifold is rare.[29–31,37] We noted that the amino group can be introduced into the NI π-system. Normally the amino group can induce red-shifted absorption.[31] Regioisomers **L-1** and **L-2** were prepared *via* the Sonogashira coupling reaction.[31] The preparation of the *N^N* Pt(II) bisacetylide complexes **Pt-1** and **Pt-2** followed the reported procedures. The known complex **Pt-0** was used as a reference compound in the study. All the compounds were obtained in moderate to good yields (see the Experimental section and ESI† for molecular structural characterization data).

UV-Vis absorption and luminescence spectra of the compounds

L-1 gives absorption at 463 nm (ε = 8900 M^{-1} cm^{-1}). **L-2** gives absorption in the blue-shifted region at 422 nm (ε = 23 600 M^{-1} cm^{-1}) (Fig. 1).

This result indicates that the effect of the regioisomer is substantial.[31] Upon complexation with the Pt(II) coordination center, **Pt-1** shows intensified absorption as compared to the ligand **L-1**, but the absorption wavelength is the same. For **L-2**, however, the absorption band moved bathochromatically upon coordination to the Pt(II) center. The absorption of both complexes is red-shifted by 50 nm compared to that of **Pt-0**.[29] To the best of our knowledge, this is the first time that amino NI acetylide is used for preparation of Pt(II) complexes. Previously we used similar ligands for preparation of cyclometalated Ir(III) complexes.[31] A similar effect was observed.

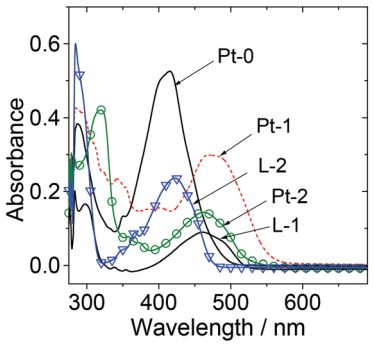

Fig. 1 UV-Vis absorption of Pt(II) complexes and ligands **L-1** and **L-2**. c = 1.0 × 10^{-5} M, in toluene, 20 °C.

The UV-Vis absorption spectra of the ligands and the complexes in solvents of different polarities were studied (Fig. 2), no substantial variation was observed. Therefore the intramolecular charge transfer of the compounds in the ground state is not significant.[14]

The photoluminescence spectra of the compounds were studied (Fig. 3). **L-2** shows emission at 422 nm and **L-1** shows emission in the red-shifted region (463 nm). Thus the regioisomerism imposes a significant effect on the photoluminescence properties of the ligands. **Pt-1** and **Pt-2** show different emission properties. The emission of **Pt-1** is stronger than that of **Pt-2**. The emission spectrum of **Pt-1** is more structured than that of **Pt-2**. Both complexes give emission at a similar wavelength (665 nm), which is slightly red-shifted compared to **Pt-0** (the energy difference is 0.12 eV).[29]

The amino-NI acetylides show much lower S_1 state energy levels than NI acetylide, by 0.85 eV and 0.46 eV for **L-2** and **L-1**, respectively. Interestingly, the T_1 state energy levels of the complexes **Pt-1** and **Pt-2** are only 0.12 eV lower than that of **Pt-0**. Higher T_1 state energy level is beneficial for the application of

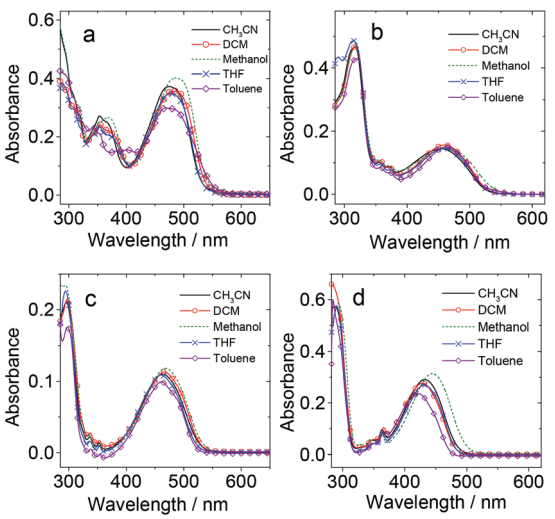

Fig. 2 UV-Vis absorption of (a) **Pt-1**, (b) **Pt-2**, (c) **L-1**, (d) **L-2** under different atmospheres in CH_3CN, DCM, methanol, THF and toluene. c = 1.0 × 10^{-5} M, 20 °C.

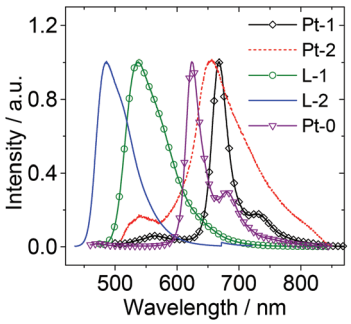

Fig. 3 The normalized emission spectra of the Pt(II) complexes and ligands: **Pt-0** (λ_{ex} = 420 nm), **Pt-1** (λ_{ex} = 495 nm), **Pt-2** (λ_{ex} = 490 nm), **L-1** (λ_{ex} = 470 nm), **L-2** (λ_{ex} = 430 nm). c = 1.0 × 10^{-5} M in toluene, 20 °C.

triplet photosensitizers because the triplet–triplet-energy-transfer (TTET) is the typical photophysical process involved in the application of the triplet photosensitizers.[5,20,38]

The luminescence of the compounds under different atmospheres was studied (Fig. 4). For both **Pt-1** and **Pt-2**, the emission in the near IR region was completely quenched in aerated solution. On the other hand, the minor emission band at 570 nm was not quenched. These results indicated that the emission in the near IR region is phosphorescence and the emission in the 500 nm–600 nm is fluorescence.

The emission of the ligands under different atmospheres was also studied (Fig. 4c and 4d). Interestingly the emission intensity is reduced in aerated solution. The assignment of the fluorescence and the phosphorescence of the compounds was supported by the measurement of the luminescence lifetimes (Table 1). For example, the luminescence lifetime of **Pt-1** and

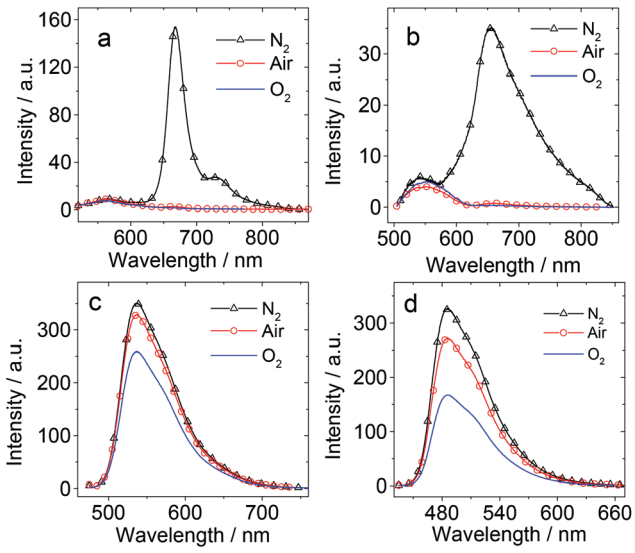

Fig. 4 The emission spectra of the Pt(II) complexes and the ligands. (a) **Pt-1** (λ_{ex} = 495 nm) (b) **Pt-2** (λ_{ex} = 490 nm), (c) **L-1** (λ_{ex} = 470 nm), (d) **L-2** (λ_{ex} = 430 nm) under different atmospheres. c = 1.0 × 10^{-5} M in toluene, 20 °C.

Pt-2 in the near IR region is 78.3 μs and 20.1 μs, respectively. The luminescence lifetime of the minor emission band in the 450 nm–550 nm region is 7.3 ns and 7.2 ns, respectively (Table 1). The minor emission band of **Pt-1** and **Pt-2** in the 450 nm–550 nm region is *unlikely* due to the impurities of the ligands because the ligands give longer fluorescence lifetimes of 10.0 ns and 9.6 ns, respectively (Table 1).

The photoluminescence spectra of the complexes in solvents of different polarities were studied (Fig. 5). **L-1** and **L-2** give different responses to the variation of solvent polarity. For example, **L-1** shows much weaker emission in CH_3CN than that in DCM. For **L-2**, however, the emission intensities in DCM and CH_3CN are similar. The luminescence of **Pt-1** and **Pt-2** in different solvents is drastically different. **Pt-1** shows a decreased emission intensity in polar solvents, but the emission variation of **Pt-2** in different solvents is more complicated. These different emission properties in different solvents can be attributed to the different intramolecular charge transfer (ICT) features of the compounds.

77 K emission spectra

In order to study the properties of the emissive triplet excited states of the complexes, the emission at 77 K was studied (Fig. 6). The emission spectra of **Pt-1** become more significant vibrational propagation, and the thermally induced Stokes shift is small. For **Pt-2**, similar emission spectra were observed at 77 K. The minor emission band in the 500 nm region was diminished. This may be due to the greatly intensified phosphorescence at 77 K as compared with that at RT. **Pt-1** and **Pt-2** share similar T_1 state energy levels (1.89 eV and 1.92 eV, respectively).

Nanosecond transient difference absorption spectroscopy

The nanosecond time-resolved transient difference absorption spectra were used to study the triplet states of the complexes (Fig. 7). Bleaching bands were found to be almost the same as the steady state UV-Vis absorption bands upon pulsed laser excitation. Moreover, similar transient absorption features were observed for **Pt-0**, **Pt-1** and **Pt-2** **in** the range of 500–700 nm which indicate the triplet states present in the ligands, while different positive transient absorption bands indicate the triplet state's difference of the ligands (**Pt-2** is much weaker than **Pt-1**). The bleaching bands of **Pt-1** and **Pt-2** are much weaker than that of **Pt-0**, which is proposed to be decreased by the strong positive transient absorption bands.

DFT calculations

To assign the triplet states of the complexes, the spin density surfaces were calculated by DFT methods.[22,39–41] Generally the triplet excited states are localized on the organic ligands, instead of the Pt(II) coordination centers (Fig. 8). This is in agreement with the long-lived triplet excited states of the complexes.

According to the calculation results of singlet–triplet state energy gaps, for **Pt-1**, the electronic component of the transition is H → L, which can be treated as the ^{3}IL transition (see

Table 1 Photophysical parameters of **Pt-0**–**Pt-2**, **L-1** and **L-2**

	λ_{abs} [a]	ε [b]	λ_{em} [c]	Φ_F [d]	Φ_P [e]	τ_F [f] (ns) 298 K	τ_F [f] (ns) 77 K	τ_P [g] (μs) 298 K	τ_P [g] (μs) 77 K	τ_T/μs [h]	Φ_Δ [i]
Pt-0	416	5.26	624	—	7.1% [j]	—	—	124 [j]	205 [j]	45.3	0.99
Pt-1	485	2.92	560, 668	0.01%	0.96%	7.3	1.4	78.3	596.9	23.7	0.84
Pt-2	465	1.43	528, 653	0.18×10^{-3}%	0.01%	7.2	2.8	20.1	457.3	0.9 [k]	0.63
L-1	463	0.89	536	23.60%	—	10.0	—	—	—	—	—
L-2	422	2.36	485	47.21%	—	9.6	—	—	—	—	—

[a] In toluene (1.0×10^{-5} mol dm^{-3}). [b] The molar extinction coefficient at the absorption maxima. ε: 10^4/cm^{-1} mol^{-1} dm^3. [c] In toluene. [d] In toluene, with DCM ($\Phi = 0.1$ in CH_2Cl_2) as the standard. [e] In toluene, DCM ($\Phi = 0.1$ in CH_2Cl_2) as the standard. [f] Luminescence lifetime, λ_{ex} = 443 nm, at RT (in deaerated toluene) and 77 K (in deaerated MTHF). [g] The phosphorescence lifetime of **Pt-1** (λ_{ex} = 495 nm) and **Pt-2** (λ_{ex} = 462 nm) at RT (in deaerated toluene) and 77 K (in deaerated MTHF). [h] Triplet state lifetime, determined by nanosecond time-resolved transient difference absorption spectroscopy, λ_{ex} = 355 nm. 1.0×10^{-5} M in deaerated toluene. [i] The quantum yield of singlet oxygen ($^1O_2$), **Pt-0** with TPP as the standard ($\Phi_\Delta = 0.62$ in CH_2Cl_2), 1.0×10^{-5} mol dm^{-3} in CH_2Cl_2. **Pt-2**–**Pt-3** with RM as the standard ($\Phi_\Delta = 0.8$ in methanol), 1.0×10^{-5} mol dm^{-3} in methanol. [j] Literature value. [k] $c = 3.0 \times 10^{-5}$ M.

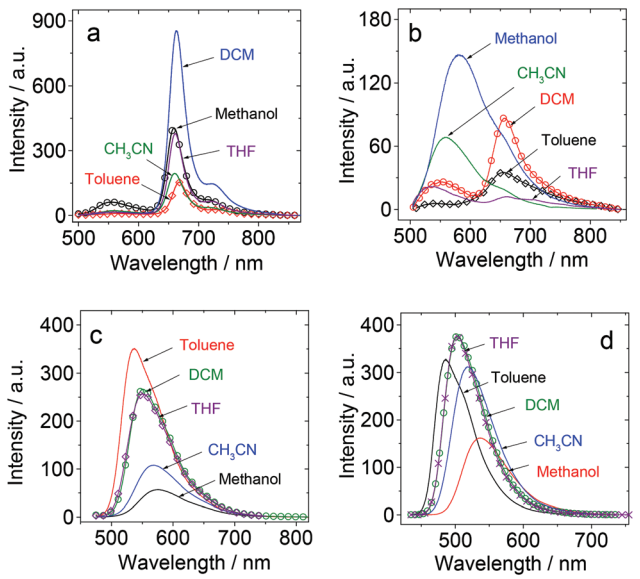

Fig. 5 The emission spectra of the Pt(II) complexes and the ligands. (a) **Pt-1** (λ_{ex} = 495 nm), (b) **Pt-2** (λ_{ex} = 490 nm), (c) **L-1** (λ_{ex} = 470 nm), (d) **L-2** (λ_{ex} = 430 nm) in different solvents. $c = 1.0 \times 10^{-5}$ M, 20 °C.

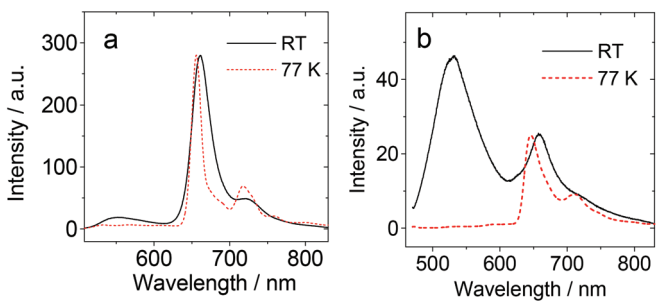

Fig. 6 Photoluminescence spectra of (a) **Pt-1** (λ_{ex} = 495 nm), (b) **Pt-2** (λ_{ex} = 462 nm) at RT and 77 K. $c = 6.0 \times 10^{-5}$ M in deaerated 2-methyl tetrahydrofuran (MTHF).

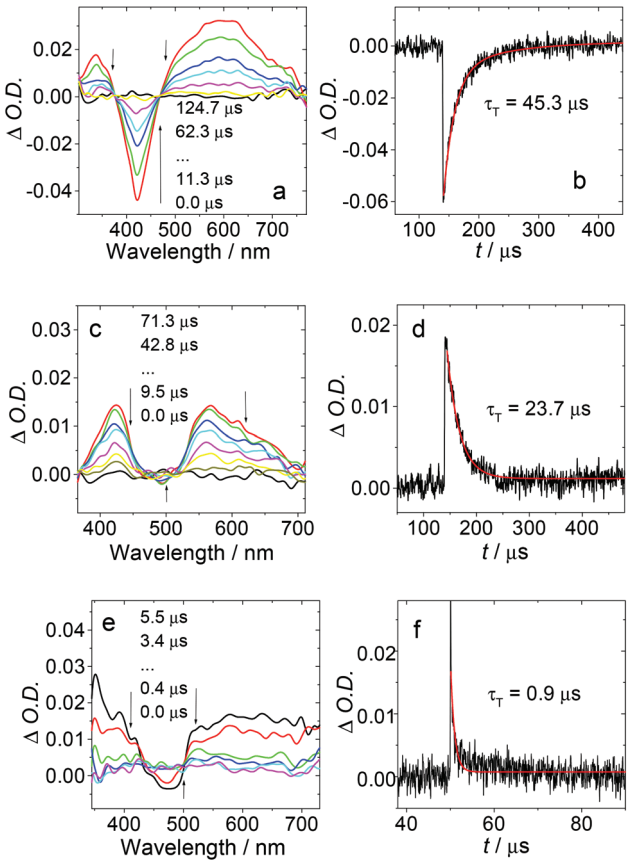

Fig. 7 Nanosecond time-resolved transient difference absorption spectra of (a) **Pt-0**, (c) **Pt-1** and (e) **Pt-2** (3.0×10^{-5} M). The decay traces were monitored at (b) **Pt-0** (540 nm), (d) **Pt-1** (560 nm), (f) **Pt-2** (550 nm, 3.0×10^{-5} M). In deaerated toluene after pulsed excitation (λ_{ex} = 355 nm). $c = 1.0 \times 10^{-5}$ M, 25 °C.

ESI†). This is in agreement with the analysis of the spin density surfaces. The predicted triplet energy level is 1.85 eV, which is close to the experimental data (1.89 eV). Similar results were also obtained for **Pt-2**, whose T_1 energy level is calculated to be 1.96 eV (the experimental value is 1.92 eV).

Triplet–triplet annihilation upconversion

The Pt(II) complexes show strong absorption of visible light and long-lived triplet excited states, thus these complexes are

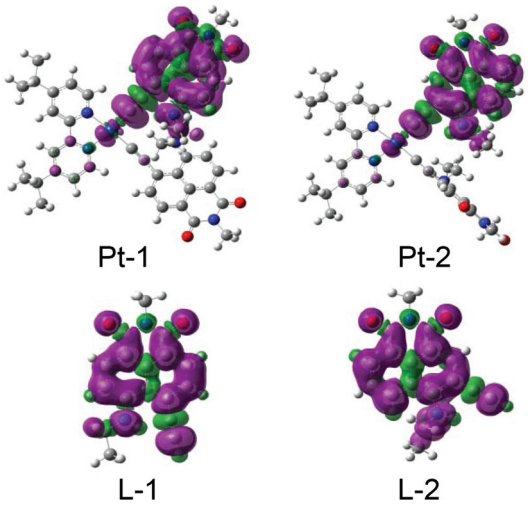

Fig. 8 Spin density of the complexes and the ligands **Pt-1**, **Pt-2**, **L-1**, **L-2**. Calculated based on the optimized triplet state by DFT at the B3LYP/6-31G(d)/LanL2DZ and CAM-B3LYP/GENECP/LanL2DZ level using Gaussian 09W.

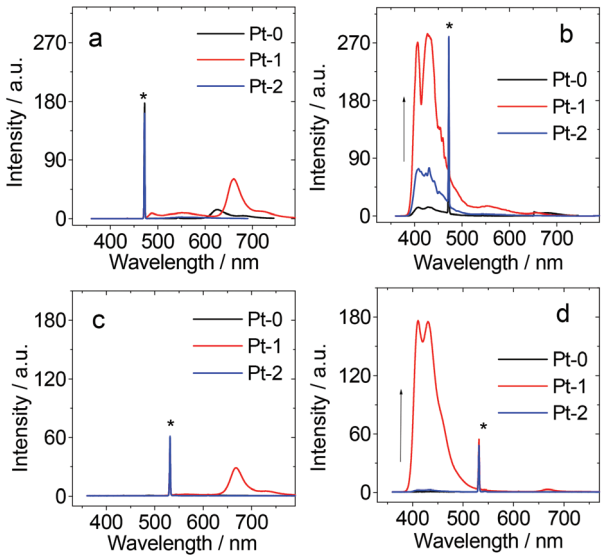

Fig. 9 Emission and upconversion of the complexes. (a) Emission of the complexes alone and (b) the upconverted DPA fluorescence and the residual fluorescence and phosphorescence of the complexes, *c* [DPA] = 4.0 × 10^{-5} M, in deaerated acetonitrile; (c) emission of the complexes alone and (d) the upconverted DPA fluorescence and the residual fluorescence and phosphorescence of the complexes, *c* [DPA] = 1.4 × 10^{-4} M, in deaerated toluene. The asterisks in (a) and (b) indicate the scattered 473 nm excitation laser (5 mW), (c) and (d) indicate the scattered 532 nm excitation laser (5 mW). *c* [sensitizers] = 1.0 × 10^{-5} M, 20 °C.

ideal triplet photosensitizers for TTA upconversion.[17,21] The crucial step of TTA upconversion, *i.e.* the TTET from the triplet photosensitizer to the triplet acceptor, can be enhanced by the strong visible light-harvesting and the long-lived triplet excited states.[21,42]

Previously a Pt(II) acetylide complex was used as a triplet photosensitizer for TTA upconversion.[43] However, the visible light-absorption of that complex was weak. Recently we used a pyrenyl acetylide Pt(II) complex for TTA upconversion.[30b] We postulate that the TTA upconversion can be improved with the new complexes **Pt-1** and **Pt-2**.

Based on the T_1 state energy levels of **Pt-1** and **Pt-2** (1.89 eV and 1.92 eV, approximated by the 77 K phosphorescence emission wavelength of **Pt-1** and **Pt-2**), 9,10-diphenyl anthracene (DPA) was selected as the triplet acceptor/emitter for which the triplet state energy level is 1.77 eV. It should be pointed out that the triplet acceptor should not show any absorption in the absorption region of the triplet photosensitizers.

Firstly the compounds were excited with a 473 nm laser (Fig. 9a). **Pt-2** shows very weak emission, but **Pt-1** shows strong emission. **Pt-0** shows much stronger emission than **Pt-2**. Upon addition of the triplet acceptor DPA, new emission bands in the blue region (400–500 nm) were observed for **Pt-1**, **Pt-2** and the reference complex **Pt-0** (Fig. 9b). However, the blue emission intensity of the three complexes varied substantially. **Pt-1** gives the strongest emission and **Pt-0** gives the weakest emission (Fig. 9b). Their different upconverted emission is attributed to their different absorption properties at the excitation wavelength. Notably **Pt-1** shows much stronger upconverted emission than **Pt-0**, although **Pt-0** has a longer T_1 state lifetime (Table 1). We also used a 532 nm laser for the photoexcitation (Fig. 9c and 9d). Only **Pt-1** can be excited and the emission at 667 nm was observed. Upon addition of DPA, **Pt-1** shows upconverted blue emission in the region of 400 nm–500 nm. **Pt-0** and **Pt-1** did not show any upconverted emission in the same region (Fig. 9d). The lack of upconverted emission of **Pt-0** and **Pt-1** is due to the inappropriate excitation wavelength. These results indicated that using amino-NI acetylides, the TTA upconversion of the complexes **Pt-1** and **Pt-2** is improved as compared to the reference complex **Pt-0**.

For the triplet–triplet upconversion quantum yields (Φ_{UC}) (Table 2), when excited with a 473 nm laser in toluene, **Pt-1** (Φ_{UC} = 0.192) is similar to **Pt-0** (Φ_{UC} = 0.199), for which the literature value is 0.181 upon excitation at 445 nm in acetonitrile. **Pt-2** (Φ_{UC} = 0.004) is much smaller than the other two complexes. It is interesting to find that the Φ_{UC} changed a lot in acetonitrile which may be due to the variation of the solvent polarity. We observed that Φ_{UC} = 0.150 and 0.011 for **Pt-1** and **Pt-2**, respectively, with 532 nm excitation in toluene. These

Table 2 Triplet excited state lifetimes (τ_T), Stern–Volmer quenching constant (K_{SV}) and bimolecular quenching constants (k_q) of the Pt(II) sensitizers. In deaerated toluene solution, 20 °C[a]

	τ_T/ μs	K_{SV}/ 10^3 M^{-1} [b]	k_q/ $10^9 M^{-1}$ s^{-1} [b]	Φ_{UC} Toluene[c]	Φ_{UC} Acetonitrile[c]	Φ_{UC} Toluene[d]
Pt-0	45.3	402.5	6.4	19.9%	3.0%	—[e]
Pt-1	23.7	50.5	2.1	19.2%	2.7%	15.0%
Pt-2	0.9	29.2	32.4	0.4%	1.9%	1.1%

[a] Upconversion quantum yields, with DCM as the standard (Φ_{UC} = 10% in CH_2Cl_2). [b] Excited at 355 nm. [c] 473 nm (5 mW) laser excitation. [d] 532 nm (5 mW) laser excitation. [e] Cannot be excited at 532 nm.

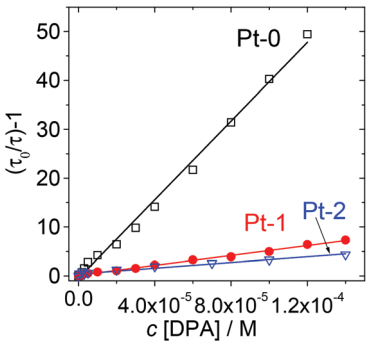

Fig. 10 Stern–Volmer plots for lifetime quenching of **Pt-0**, **Pt-1** and **Pt-2** with increasing concentration of DPA. *c* [photosensitizers] = 1.0×10^{-5} M, in deaerated toluene, 20 °C.

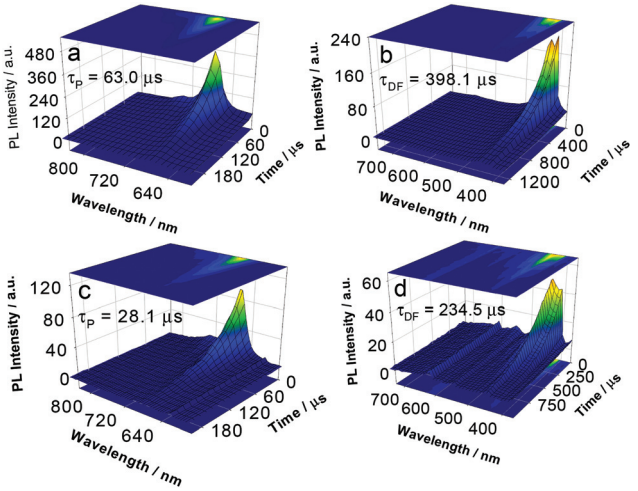

Fig. 11 Time-resolved emission spectra (TRES) of **Pt-1** alone and the TTA upconversion. With DPA as the triplet acceptor. (a) **Pt-1** alone, the phosphorescence region was measured (600 nm–830 nm, τ = 63.0 µs). (b) TRES of **Pt-1** in the presence of DPA. Upconverted emission in the range of 400 nm–500 nm was observed (τ = 398.1 µs). (c) **Pt-2** alone, the phosphorescence region was measured (580 nm–830 nm, τ = 28.1 µs). (d) TRES of **Pt-2** in the presence of DPA. Upconverted emission in the range of 400 nm–500 nm was observed (τ = 234.5 µs). *c* [DPA] = 1.4×10^{-4} M; *c* [sensitizers] = 1.0×10^{-5} M. In deaerated toluene. Excited with a nanosecond pulsed OPO laser synchronized with a spectrofluorometer (λ_{ex} = 532 nm), 25 °C.

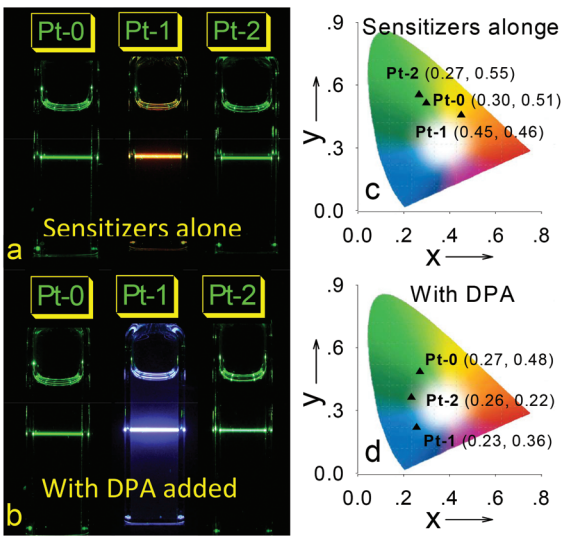

Fig. 12 (a) Photographs of the emission of sensitizers alone and (b) the upconversion. (c) CIE diagram of the emission of sensitizers alone and (d) in the presence of DPA (upconversion). λ_{ex} = 532 nm (laser power: 5 mW). **Pt-0** cannot be excited by a 532 nm laser. In deaerated toluene, *c*[sensitizer] = 1.0×10^{-5} M, *c*[DPA] = 1.4×10^{-4} M, 20 °C.

results indicate different effects of the ligands on the photophysics of the complexes.

In order to study the TTET process of the TTA upconversion of the complexes, the quenching of the triplet state lifetimes of the complexes by the triplet acceptor DPA was studied (Fig. 10). **Pt-0** gives much larger quenching constants than **Pt-1** and **Pt-2**. However, the upconversion of **Pt-0** is the weakest among the three complexes. These results indicated that the visible light-harvesting ability of the triplet photosensitizer is crucial for the triplet photosensitizers used for TTA upconversion.

In order to unambiguously confirm that the TTA upconversion is responsible for the blue emission band of the triplet photosensitizer/DPA mixed samples, the time-resolved emission spectra (TRES) were recorded (Fig. 11). For **Pt-1** alone, long-lived emission at 667 nm was observed, with a lifetime of 63.0 µs. For the mixture **Pt-1**/DPA, however, the emission band at 660 nm was quenched, and a new emission band in the 400 nm region developed. The lifetime of the emission is 398.1 µs. This long-lived fluorescence emission is the characteristic feature of the TTA upconversion. Similar TRES was observed for **Pt-2**. The luminescence lifetime of **Pt-2** alone was determined as 28.1 µs. In the presence of DPA, however, the emission band at 410 nm with a lifetime of 234.5 µs was observed.

The upconverted emission is visible to the unaided eye (Fig. 12). The photographs of the emission of the triplet photosensitizers alone and in the presence of DPA (TTA upconversion) were taken (Fig. 12). With 532 nm laser excitation, only **Pt-1** shows phosphorescence emission. With addition of DPA, strong blue emission was observed for **Pt-1**. For **Pt-2**, however, no upconverted blue emission was observed.

The efficiency of the triplet excited state production is studied by photosensitizing singlet oxygen ($^1O_2$) with the complexes (Table 3 and Fig. 13). 1,5-Dihydroxylnaphthalene (DHN) was photooxidized with the complexes as the photosensitizers.[44,45] The progress of the photooxidation is monitored by UV-Vis absorption changes. The absorption of DHN at 301 nm decreased as well as that of the oxidation product juglone at 427 nm increased due to the consumption of DHN and the production of juglone. More significant changes of UV-Vis absorption were found for **Pt-1** than that for **Pt-2**.

The photooxidation kinetics was studied by plotting the $\ln(C_t/C_0)$ against the irradiation time. Similar results were obtained that **Pt-1** has a steeper slope than **Pt-2**. These results

Table 3 Photophysical parameters of the Pt(II) and the organic triplet photosensitizers[a]

	k_{obs}/min^{-1} [a]	v_i [b]	Yield[c] (%)	Φ_Δ [d]
Pt-0	47.4	4.74	81.9	0.99
Pt-1	45.0	4.50	82.2	0.84
Pt-2	16.3	1.63	62.6	0.63
MB	43.5	4.35	81.5	0.57[e]
TPP	53.9	5.39	82.9	0.62[e]
RB	78.6	7.86	60.5	0.80[e]
Ir(ppy)$_2$bpy	2.2	0.22	23.3	—

[a] Photoreaction rate constants, 10^{-3} min^{-1}. [b] Initial rate, 10^{-6} M, in min^{-1}. [c] The yield of juglone after photoirradiation for 40 min. [d] The quantum yield of singlet oxygen ($^1O_2$), with TPP (for **Pt-0** Φ_Δ = 0.62 in CH_2Cl_2) and Rose Bengal (RB) (for **Pt-1** and **Pt-2** Φ_Δ = 0.80 in methanol) as standards. [e] Literature values.

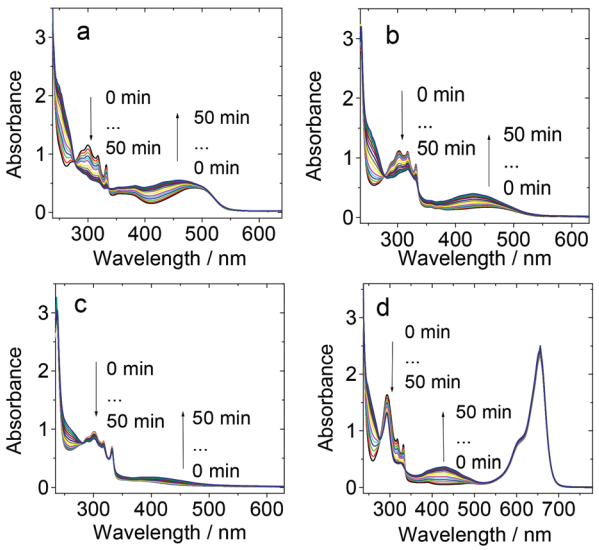

Fig. 13 Photosensitizing of $^1O_2$ with the complexes as photosensitizers. Irradiation time-dependent decrease of absorbance at 301 nm of DHN (1.0×10^{-4} M) with different $^1O_2$ sensitizers (a) **Pt-1**, (b) **Pt-2**, (c) **Ir(ppy)$_2$bpy**, (d) **MB**. *c* [sensitizers] = 1.0×10^{-5} M. In CH_2Cl_2–MeOH (9 : 1, v/v), 12 mW cm^{-2}, 20 °C.

indicated different effects of the two ligands on the photooxidation ability. What is more, **Pt-1** gives a similar slope to **Pt-0**, even steeper than the typical photosensitizer methylene blue (MB). **Pt-0**, **Pt-1** and MB gave similar results which are much higher than **Pt-2**.

The Φ_Δ values of 0.84 and 0.61 were determined for **Pt-1** and **Pt-2**, respectively. The high Φ_Δ values of **Pt-1** indicate their high photooxidation ability (Fig. 14).

Conclusions

In conclusion, two *N^N* Pt(II) bis(acetylide) complexes **Pt-1** and **Pt-2** with regioisomeric amino naphthalimide acetylide ligands (**L-1** and **L-2**, **L-1** = 5-amino-4-ethyl naphthaleneimide; **L-2** = 3-amino-4-ethyl naphthaleneimide) were prepared. The

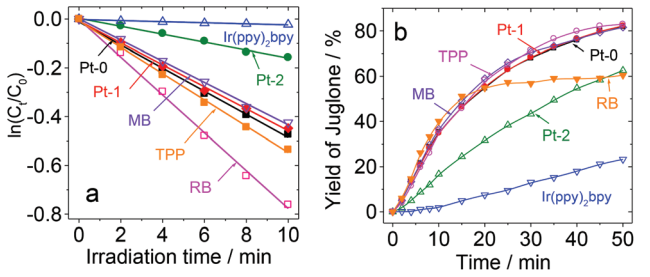

Fig. 14 Photosensitizing of $^1O_2$ with the complexes as photosensitizers. Irradiation time-dependent decrease of absorbance at 301 nm of DHN (1.0×10^{-4} M) with different $^1O_2$ sensitizers. (a) Plots of ln (C_t/C_0) *vs.* irradiation time. (b) Plots of the chemical yield as a function of irradiation time for the photooxidation of DHN. *c* [sensitizers] = 1.0×10^{-5} M. In CH_2Cl_2–MeOH (9 : 1, v/v), 20 °C.

two complexes show red-shifted absorption in the 450–550 nm region, as well as a long-lived triplet excited state (23.7 μs) as compared with the previously reported Pt(II) complexes (the T_1 state lifetime is less than 5 μs). The complexes were used as triplet photosensitizers for triplet–triplet annihilation (TTA) upconversion. An improved upconversion quantum yield (up to 15.0%) was observed. The two complexes with regioisomeric ligands show distinctly different photophysical properties, such as the maximal absorption wavelength (485 nm *vs.* 465 nm), triplet excited state lifetimes (23.7 μs *vs.* 0.9 μs), solvent-polarity dependence of the emission properties and TTA upconversion quantum yields (15.0% *vs.* 1.1%). Our results are useful for designing new visible light-harvesting Pt(II) bisacetylide complexes as triplet photosensitizers which can be used in areas such as photocatalysis, photodynamic therapy, and TTA upconversion.

Acknowledgements

We thank the NSFC (21073028, 21273028 and 91127005), the Royal Society (UK) and NSFC (Cost-Share-21011130154), the Ministry of Education (SRFDP-20120041130005), the Program for Changjiang Scholars and Innovative Research Team in University [IRT_13R06], the State Key Laboratory of Fine Chemicals (KF1203), the Fundamental Research Funds for the Central Universities (DUT14ZD226) and the Dalian University of Technology (DUT2013TB07) for financial support.

Notes and references

1 J. A. G. Williams, *Top. Curr. Chem.*, 2007, **281**, 205–268.
2 K. K.-W. Lo, A. W.-T. Choi and W. H.-T. Law, *Dalton Trans.*, 2012, **41**, 6021–6047.
3 Q. Zhao, F. Li and C. Huangm, *Chem. Soc. Rev.*, 2010, **39**, 3007–3030.
4 Y. Feng, J. Cheng, L. Zhou, X. Zhou and H. Xiang, *Analyst*, 2012, **137**, 4885–4901.

5 H. Xiang, J. Cheng, X. Ma, X. Zhou and J. J. Chruma, *Chem. Soc. Rev.*, 2013, **42**, 6128–6185.
6 D.-L. Ma, V. P.-Y. Ma, D. S.-H. Chan, K.-H. Leung, H.-Z. He and C.-H. Leung, *Coord. Chem. Rev.*, 2012, **256**, 3087–3113.
7 F. N. Castellano, I. E. Pomestchenko, E. Shikhova, F. Hua, M. L. Muro and N. Rajapakse, *Coord. Chem. Rev.*, 2006, **250**, 1819–1828.
8 X. Wang, S. Goeb, Z. Ji, N. A. Pogulaichenko and F. N. Castellano, *Inorg. Chem.*, 2011, **50**, 705–707.
9 L. Shi and W. Xia, *Chem. Soc. Rev.*, 2012, **41**, 7687–7697.
10 S. Suzuki, R. Sugimura, M. Kozaki, K. Keyaki, K. Nozaki, N. Ikeda, K. Akiyama and K. Okada, *J. Am. Chem. Soc.*, 2009, **131**, 10374–10375.
11 V. F. Moreira, F. L. T. Greenwood and M. P. Coogan, *Chem. Commun.*, 2010, **46**, 186–202.
12 A. Y.-Y. Tam and V. W.-W. Yam, *Chem. Soc. Rev.*, 2013, **42**, 1540–1567.
13 E. Baggaley, J. A. Weinstein and J. A. G. Williams, *Coord. Chem. Rev.*, 2012, **256**, 1762–1785.
14 F. Guo and W. Sun, *J. Phys. Chem. B*, 2006, **110**, 15029–15036.
15 R. Liu, A. Azenkeng, Y. Li and W. Sun, *Dalton Trans.*, 2012, **41**, 12353–12357.
16 T. N. Rachford and F. N. Castellano, *Coord. Chem. Rev.*, 2010, **254**, 2560–2573.
17 J. Zhao, S. Ji and H. Guo, *RSC Adv.*, 2011, **1**, 937–950.
18 P. Ceroni, *Chem. – Eur. J.*, 2011, **17**, 9560–9564.
19 Y. C. Simon and C. Weder, *J. Mater. Chem.*, 2012, **22**, 20817–20830.
20 J. Zhao, W. Wu, J. Sun and S. Guo, *Chem. Soc. Rev.*, 2013, **42**, 5323–5351.
21 J. Zhao, S. Ji, W. Wu, W. Wu, H. Guo, J. Sun, H. Sun, Y. Liu, Q. Li and L. Huang, *RSC Adv.*, 2012, **2**, 1712–1728.
22 W. Wu, J. Zhao, H. Guo, J. Sun, S. Ji and Z. Wang, *Chem. – Eur. J.*, 2012, **18**, 1961–1968.
23 W. Wu, J. Sun, X. Cui and J. Zhao, *J. Mater. Chem. C*, 2013, **1**, 4577–4589.
24 J. Sun, F. Zhong, X. Yi and J. Zhao, *Inorg. Chem.*, 2013, **52**, 6299–6310.
25 X. Yi, J. Zhao, J. Sun, S. Guo and H. Zhang, *Dalton Trans.*, 2013, **42**, 2062–2074.
26 X. Yi, J. Zhao, W. Wu, D. Huang, S. Ji and J. Sun, *Dalton Trans.*, 2012, **41**, 8931–8940.
27 A. A. Rachford, S. Goeb and F. N. Castellano, *J. Am. Chem. Soc.*, 2008, **130**, 2766–2767.
28 I. E. Pomestchenko, C. R. Luman, M. Hissler, R. Ziessel and F. N. Castellano, *Inorg. Chem.*, 2003, **42**, 1394–1396.
29 H. Guo, M. L. M. Small, S. Ji, J. Zhao and F. N. Castellano, *Inorg. Chem.*, 2010, **49**, 6802–6804.
30 (*a*) H. Guo, S. Ji, W. Wu, W. Wu, J. Shao and J. Zhao, *Analyst*, 2010, **135**, 2832–2840; (*b*) S. Ji, W. Wu, J. Zhao, H. Guo and W. Wu, *Eur. J. Inorg. Chem.*, 2012, **19**, 3183–3190.
31 L. Ma, S. Guo, J. Zhao and H. Guo, *Chin. Sci. Bull. (Chin Ver)*, 2014, **59**, 1655–1666.
32 M. J. Frisch, G. W. Trucks, H. B. Schlegel, G. E. Scuseria, M. A. Robb, J. R. Cheeseman, G. Scalmani, V. Barone, B. Mennucci, G. A. Petersson, H. Nakatsuji, M. Caricato, X. Li, H. P. Hratchian, A. F. Izmaylov, J. Bloino, G. Zheng, J. L. Sonnenberg, M. Hada, M. Ehara, K. Toyota, R. Fukuda, J. Hasegawa, M. Ishida, T. Nakajima, Y. Honda, O. Kitao, H. Nakai, T. Vreven, J. A. Montgomery Jr., J. E. Peralta, F. Ogliaro, M. Bearpark, J. J. Heyd, E. Brothers, K. N. Kudin, V. N. Staroverov, R. Kobayashi, J. Normand, K. Raghavachari, A. Rendell, J. C. Burant, S. S. Iyengar, J. Tomasi, M. Cossi, N. Rega, J. M. Millam, M. Klene, J. E. Knox, J. B. Cross, V. Bakken, C. Adamo, J. Jaramillo, R. Gomperts, R. E. Stratmann, O. Yazyev, A. J. Austin, R. Cammi, C. Pomelli, J. W. Ochterski, R. L. Martin, K. Morokuma, V. G. Zakrzewski, G. A. Voth, P. Salvador, J. J. Dannenberg, S. Dapprich, A. D. Daniels, Ö. Farkas, J. B. Foresman, J. V. Ortiz, J. Cioslowski and D. J. Fox, *GAUSSIAN 09W(Revision A.1)*, Gaussian Inc., Wallingford CT, 2009.
33 X. Lu, W. Zhu, Y. Xie, X. Li, Y. Gao, F. Li and H. Tian, *Chem. – Eur. J.*, 2010, **16**, 8355–8364.
34 S. V. Bhosale, C. Jani, C. H. Lalander and S. J. Langford, *Chem. Commun.*, 2010, **46**, 973–975.
35 T. D. M. Bell, S. Yap, C. H. Jani, S. V. Bhosale, J. Hofkens, F. C. De Schryver, S. J. Langford and K. P. Ghiggino, *Chem. – Asian J.*, 2009, **4**, 1542–1550.
36 F. Chaignon, M. Falkenström, S. Karlsson, E. Blart, F. Odobel and L. Hammarström, *Chem. Commun.*, 2007, 64–66.
37 J. Sun, W. Wu and J. Zhao, *Chem. – Eur. J.*, 2012, **18**, 8100–8112.
38 Y. You and W. Nam, *Chem. Soc. Rev.*, 2012, **41**, 7061–7084.
39 K. Hanson, A. Tamayo, V. V. Diev, M. T. Whited, P. I. Djurovich and M. E. Thompson, *Inorg. Chem.*, 2010, **49**, 6077–6084.
40 W. Wu, J. Zhao, J. Sun and S. Guo, *J. Org. Chem.*, 2012, **77**, 5305–5312.
41 Y. Liu and J. Zhao, *Chem. Commun.*, 2012, **48**, 3751–3753.
42 A. Monguzzi, R. Tubino, S. Hoseinkhani, M. Campione and F. Meinardi, *Phys. Chem. Chem. Phys.*, 2012, **14**, 4322–4332.
43 P. Du and R. Eisenberg, *Chem. Sci.*, 2010, **1**, 502–506.
44 S.-Y. Takizawa, R. Aboshi and S. Murata, *Photochem. Photobiol. Sci.*, 2011, **10**, 895–903.
45 J. Sun, J. Zhao, H. Guo and W. Wu, *Chem. Commun.*, 2012, **48**, 4169–4171.

